Supporting Online Material

Principal components analysis of genetic data

PCA can be conducted on population genetic data in at least two major ways; either in a population-based or individual-based manner. The two approaches differ in how the input data matrix for PCA is defined, but once this matrix is defined, the steps are identical. Let G represent the input data matrix, and let it have n rows and m columns.

For our population-based results, we used a data matrix with one row for each of n pre-defined populations, and one column for each of m bi-allelic loci. The element $G(i, j)$ is initially set to the frequency of the derived allele at the jth locus in the ith population. The columns of the matrix are then mean-centered by subtracting from each element the mean of the elements in that column (so that after normalization, the column means equal zero). Following Cavalli-Sforza et al, we do not further normalize the columns.

For the individual-based approach, there are no pre-defined populations, and the data matrix G has one row for each of n individuals and one column for each of m loci. The element $G(i, j)$ is then set to an integer representing the number of copies of the derived allele found in individual i at locus j (so that for autosomal data, the entries are 0,1, or 2). Let $\mu(j)$ be the mean of the jth column and $p(j)$ be the maximum likelihood estimate of the allele frequency for that column (i.e. $p(j) = \mu(j)/2$). Following [1] the matrix G is then normalized by subtracting from element $G(i, j)$ the column mean $\mu(j)$ and then dividing by $\sqrt{p(j)(1 - p(j))}$.

In the individual-based approach, we make a slight variation for autosomal dominant markers (e.g. AFLPs). For autosomal dominant markers, we define an indicator variable $I(i, j)$, that takes the value 0 (or 1) if an AFLP band is absent (or present) for marker j in individual i. We initially set $G(i, j)$ equal to $I(i, j)$. We then compute the column means $\mu(j)$ and column standard deviations $\sigma(j)$. We then normalize the matrix by subtracting from $G(i, j)$ the column mean $\mu(j)$ and then dividing by $\sigma(j)$, the observed standard deviation.

Given the $n \times m$ data matrix G, the first step of PCA is to compute the $n \times n$ sample covariance matrix X among the units of interest (i.e. populations or individuals):

$$X = \frac{1}{n} G G'$$

where G' denotes the transpose of G. Some examples of covariance matrices from simulated data are given in fig. S3.

The second step is to compute the eigenvectors of X. The kth eigenvector will be of length n with one entry for each individual/population. When geographical coordinates are available for each individual/population, each eigenvector entry is then naturally associated with a particular geographical coordinate, and a contour plot or heat map can be made to show how the eigenvector values vary across geographical space (Specifically, in our manuscript the kth PC-map is a heat map showing how the entries in the kth eigenvector vary across geographical space). When geographical coordinates are not available, a common visualization strategy is to plot the corresponding elements of one eigenvector against another, producing biplots as in fig. 2 for example.

Simulation details

To generate both individual and population-based data (as described in the Methods Summary), we used Hudson's `ms` software [2]. To simulate L polymorphic loci, we independently simulate L loci with the number of segregating sites per locus fixed to 1.

For the results of the two-dimensional population-based simulations shown in fig. 1, $n = 100$, $D_s = 15 \times 15$, $D = 31 \times 31$, $L = 500$, $4Nm = 0.1$. For the one-dimensional individual-based results of fig. 2, the parameters used were $n = 50$, $D = 100$, $L = 1000$, $4Nm = 1$.

We also simulated data using an alternative Gaussian-process-based spatial model for allele frequencies (originally described in [3]). We observed similar sinusoidal patterns in PCs computed from these data to those we observed in the explicit population genetic simulations using `ms` (results not shown). This is as predicted by theory (see main paper) as both models induce a spatial covariance structure among sampled individuals, with genetic similarity tending to decay with distance.

Color-coding of Cavalli-Sforza et al's original PCA maps

Figures 3.11.1-3.11.4, 4.17.1-4.17.5, and 5.11.1-5.11.4 from the "History and Geography of Human Genes" were scanned in using Adobe Photoshop software. Fig. S12 provides an example of one of the original images. Adobe Illustrator CS2's LiveTrace feature was used to create vector-based representations of each scanned image. Some minor errors in original plots are introduced by this step but they are only very fine-scale errors in small regions of the graphs. The hash marks that denote contour plot level intensities in the original images were deleted manually using the Selection tool. The LivePaint feature was used to fill each contour region with colors meant to represent the eight levels used in Cavalli-Sforza's original plots. Specifically, we used a CMYK color model with the C and K components set to 100%, K set to 100%, and values of M that vary along a uniform interval between 0 and 100%. In five cases to make the similarity among PC plots more clear, the ordering of the levels was reversed from that in the original Cavalli-Sforza plot (i.e., Africa PC1 & PC4, Asia PC1, PC2, and PC5). Because PCs are arbitrary with respect to having a positive/negative sign, reversing the order of the levels does not represent a distortion of the original PCA results.

Analysis of *Phylloscopus trochiloides* (Greenish warblers) data

To examine the behavior of PCA of spatial data in an empirical context, we applied PCA to a previously published dataset [4] of amplified fragment length polymorphism (AFLP) data from greenish warblers (*Phylloscopus trochiloides*). Greenish warblers are of broader interest because they are a well-documented example of a ring species complex [5, 4]. Greenish warblers are most abundant in western and eastern Siberia. Where these two main populations overlap geographically, there is no mating between the two, yet the two populations are connected by gene flow via a narrow band of populations to the south that are arranged in a ring around the Tibetan plateau. While this species is distributed along a ring, because the warblers do not interbreed across the top of the ring, greenish warblers can be thought of as inhabiting a one-dimensional habitat. Thus for our purposes, greenish warblers are an interesting test case for our results regarding PCA in one-dimensional habitats.

The data collected by Irwin et al [4] consist of 62 AFLP markers typed on 105 individuals from 26 geographic sites. AFLPs are dominant markers, so each marker is typed for presence or absence. Irwin et al also conducted PCA on this data and plotted PC1 against distance along the ring; however our analysis differs in a few ways. We normalized each AFLP variable to have a standard unit variance before applying PCA (similar to [6]), we excluded five sites that are outside of the central ring (GT,FN,NZ,TU, and YK), and we calculated position along the ring in a different manner. To calculate position of each individual along the ring we fit an ellipse to the geographic distribution of sampling sites and then mapped each site onto the ellipse, and took the distance from an arbitrary point on the ellipse as an indicator of position.

If covariance between each individual's AFLP markers decays with distance and sampling error is small, we expect sinusoidal patterns would emerge in the PCA results. Indeed, biplots for PC1 and PC2 (fig. S10) revealed the horseshoe-shaped Lissajous pattern that is expected when plotting a roughly linear gradient for PC1 against a quadratic form for PC2 (as in fig. 2). In agreement with our simulation results (eg, fig. 2) PC1 is directly related to location within the one-dimensional habitat and PC2 is related to distance from the center of the 1-dimensional habitat (fig. S9). These patterns were also observed if we treated each sampling location as a population and used population-based PCA on the data (results not shown).

These results are consistent with arguments made by Irwin et al. regarding the presence of isolation-by-distance in this system. PC3 (fig. S9) does not have a clear relationship to geography, rather it appears to account mainly for variation among individuals sampled from Eastern Siberia. Subsequent PCs (data not shown) appear noisy with no clear geographical relationship. This is consistent with a result we found in simulations, that for smaller datasets (in terms of both number of loci and individuals) the higher principal components are typically too noisy to recognize the sinusoidal-like patterns.

Selection of PCs in controlling for population structure

One practical issue regarding PCA-based approaches to controlling for population structure in association studies is deciding which PCs to use. Although in simulations for a discrete 2-population model Price et al [7] found results to be relatively robust to which PCs are used, in general omitting relevant PCs may fail to fully control for structure (e.g. produce an elevated type I error), whereas including irrelevant PCs would be expected to reduce power. One suggestion in [7] is to select PCs based on the"significance" of their eigenvalue [6]. In spatially continuous populations, given enough data, we expect the number of significant eigenvalues to be large. This is because individuals sampled from a continuous population can be thought of as being drawn from a large number of discrete subpopulations exchanging migrants, and for discrete population models, given enough data, the number of "significant" eigenvalues/PCs is one less than the number of subpopulations [6]. (In practice, limits on available amounts of data would be expected to yield fewer significant eigenvalues.) For the example shown in fig. 2 (a sample of 1000 SNPs from 50 individuals from a linear set of 100 demes with effective migration rate $4Nm = 1$), we found using the method of [6] that 12 eigenvalues (of a possible maximum of 49) are "significant" at $p < 0.05$ (fig. S2). If some of these significant PCs are not correlated with phenotype (once other PCs have been controlled for) then controlling for them is unnecessary, and may reduce power. This suggests that the problem of appropriately choosing the number of PCs may warrant further consideration, and we suggest that an attractive solution to this problem should involve considering whether eigenvectors are correlated with phenotype.

References

[1] Patterson, N., Price, A. L., and Reich, D. *PLoS Genet* **2**(12), e190 (2006).

[2] Hudson, R. R. *Bioinformatics* **18**(2), 337–8 (2002).

[3] Wasser, S. K., Shedlock, A. M., Comstock, K., Ostrander, E. A., Mutayoba, B., and Stephens, M. *Proc Natl Acad Sci U S A* **101**, 14847–52 (2004).

[4] Irwin, D. E., Bensch, S., Irwin, J. H., and Price, T. D. *Science* **307**(5708), 414–6 (2005).

[5] Irwin, D. E., Bensch, S., and Price, T. D. *Nature* **409**(6818), 333–7 (2001).

[6] Patterson, N., Price, A., and Reich, D. *PLoS Genet* **2**(12), e190 (2006).

[7] Price, A. L., Patterson, N. J., Plenge, R. M., Weinblatt, M. E., Shadick, N. A., and Reich, D. *Nat Genet* **38**(8), 904–9 (2006).

[8] Cavalli-Sforza, L. L., Menozzi, P., and Piazza, A. *The History and Geography of Human Genes.* Princeton University Press, (1994).

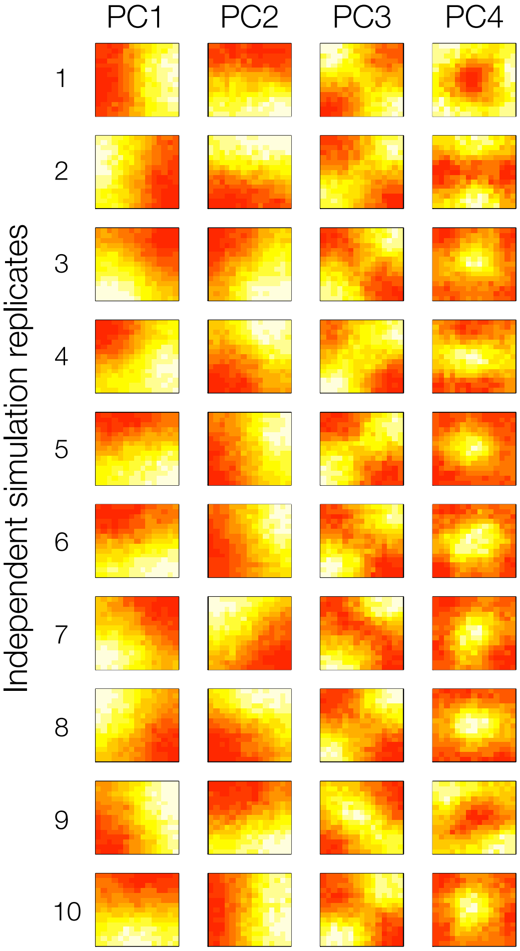

Figure S1: **Plots of the first four PC-maps for 10 independent simulation replicates where there is constant homogeneous migration in a 2-dimensional habitat.** Parameters are the same as in fig. 1 of the main text, i.e. $4Nm = 0.1$, $D_s = 225$ (i.e., 15×15), $D = 961$ (i.e., 31×31), $n = 200$, and $L = 500$. Noteworthy features include: (1) the exact angle of the gradient in PC1 varies across runs but PC1 is consistently a gradient across the habitat and PC2 is consistently a perpendicular gradient to that of PC1. (2) PC3 is typically a saddle-like shape. (4) PC4 is typically a mound- or bowl-like shape (note: the sign of the PC is arbitrary, so whether one views the shape as a mound or bowl is arbitrary). (5) The order of PC patterns sometimes fluctuates: In replicate 2, PC4 has changed order with the PC-map that is typically expected as PC5, so that the mound-like shape is present in the PC5 map (not shown). This re-ordering of the PCs occurs more frequently when smaller numbers of individuals or loci are used (not shown). (6) In addition to the overall similarity of results across independent replicates, in many cases replicates show similarity in detail (e.g. PC1 gradients that are in the same direction). For instance, replicates 4,5,6, and 8 all show a ”north-west / south-east” gradient in PC1 even though the individual histories of migration in each simulation are independent of one another. Amongst all 45 possible pairwise comparisons ∼10 show roughly equivalent patterns for PC1 and PC2 [e.g. pairs (1-2),(3-7),(3-9),(4-5),(4-6),(4-8),(5-6),(5-8),(6-8),(7-9)]

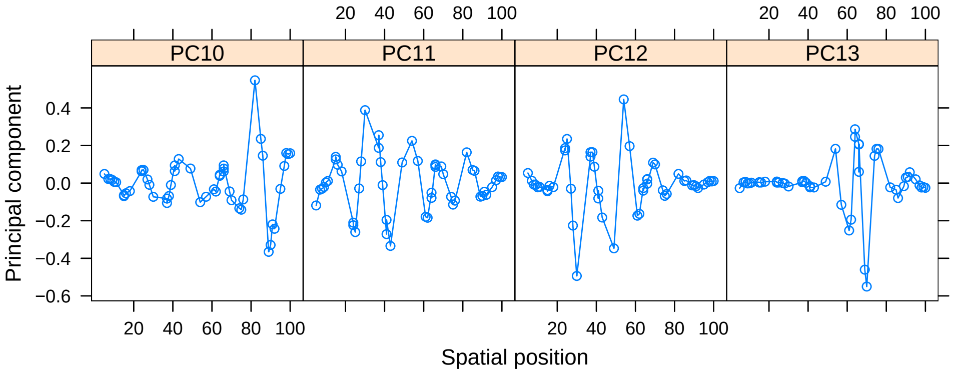

Figure S2: **One-dimensional PC-maps for PCs 10-13 for the same case as in fig. 2 in the main text.** PC12 is the last "significant" axis of variation according to the method of [6]. Parameters for these individual-based simulations are: $n = 50$, $D = 100$, $4Nm = 1$ and $L = 1000$.

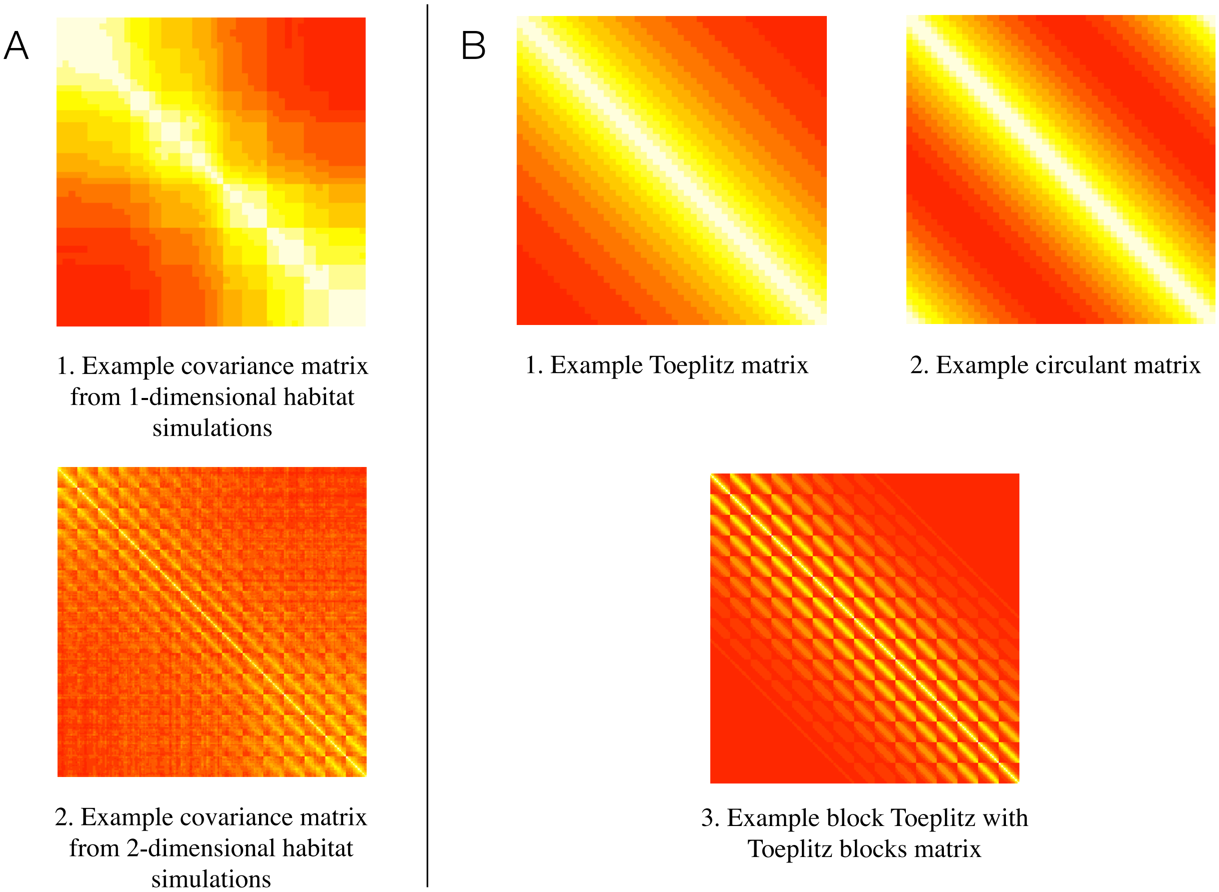

1. Example covariance matrix from 1-dimensional habitat simulations

2. Example covariance matrix from 2-dimensional habitat simulations

1. Example Toeplitz matrix

2. Example circulant matrix

3. Example block Toeplitz with Toeplitz blocks matrix

Figure S3: **Examples of the major classes of matrices referred to in the main text.** The matrices are depicted by coloring each element of each matrix in proportion to the magnitude of the value in the element, where whiter colors represent larger values. **Panel A: Examples of sample covariance matrices from simulated data.** For (A1) the rows of the covariance matrix are ordered by the geographic position of each individual and the simulated data are from the simulations shown in fig. 2 of the main text. The decrease in values as one moves away from the matrix diagonal reflects how covariance decays with distance between individuals (note though that the data also show a boundary effect that increases covariance among individuals near either end of the habitat). For (A2) the rows of the covariance matrix are also ordered by the geographic position of the individuals in the 2-d habitat (such that individuals are ordered from "west" to "east" and then from "north" to "south"). Specifically, this covariance matrix corresponds to the simulated data used in fig. 1 of the main text and it also shows a general decay of covariance with distance. **Panel B: Structured matrices that arise from idealized scenarios (see main text).** Theoretical results presented in the main text relate to the example toeplitz (B1), circulant (B2), and block Toeplitz with Toeplitz block matrices (B3). Of particular importance is how (A1) shows a similar structure to a Toeplitz matrix (B1) for which theoretical results are available and likewise (A2) shows a similar structure to a block Toeplitz with Toeplitz blocks matrix (B3).

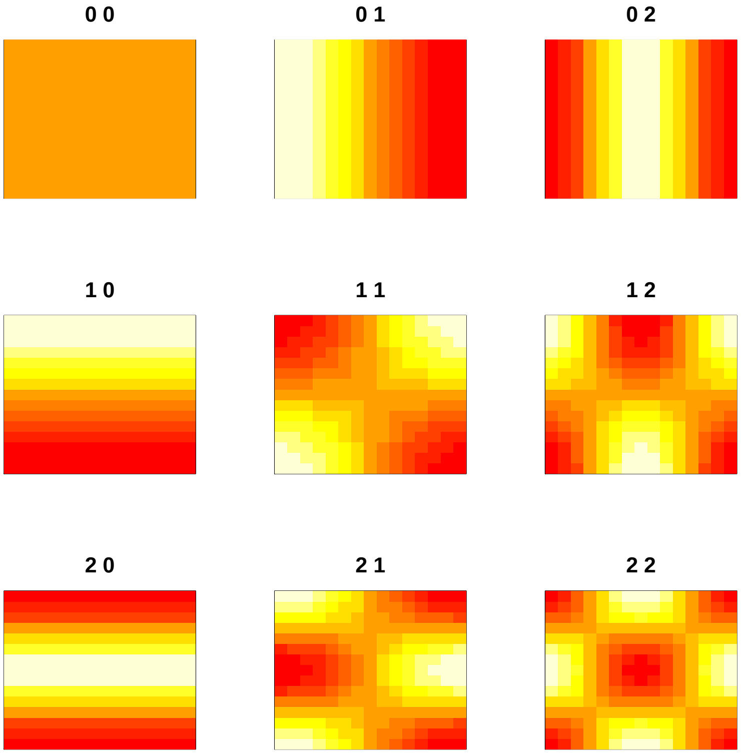

Figure S4: **Plots of 9 basis functions of the two-dimensional Discrete Cosine Transform (DCT) for 15×15 sample points.** The i, jth element of each plot is equal to $\cos(\frac{2\pi(2i+1)u}{2 \cdot 15})\cos(\frac{2\pi(2j+1)v}{2 \cdot 15})$, where u and v are given as an ordered pair above the image. To obtain the complete set of 15^2 basis functions, one must take the corresponding plots for all possible ordered pairs of $u = 0 \ldots, 14$ and $v = 0 \ldots, 14$.

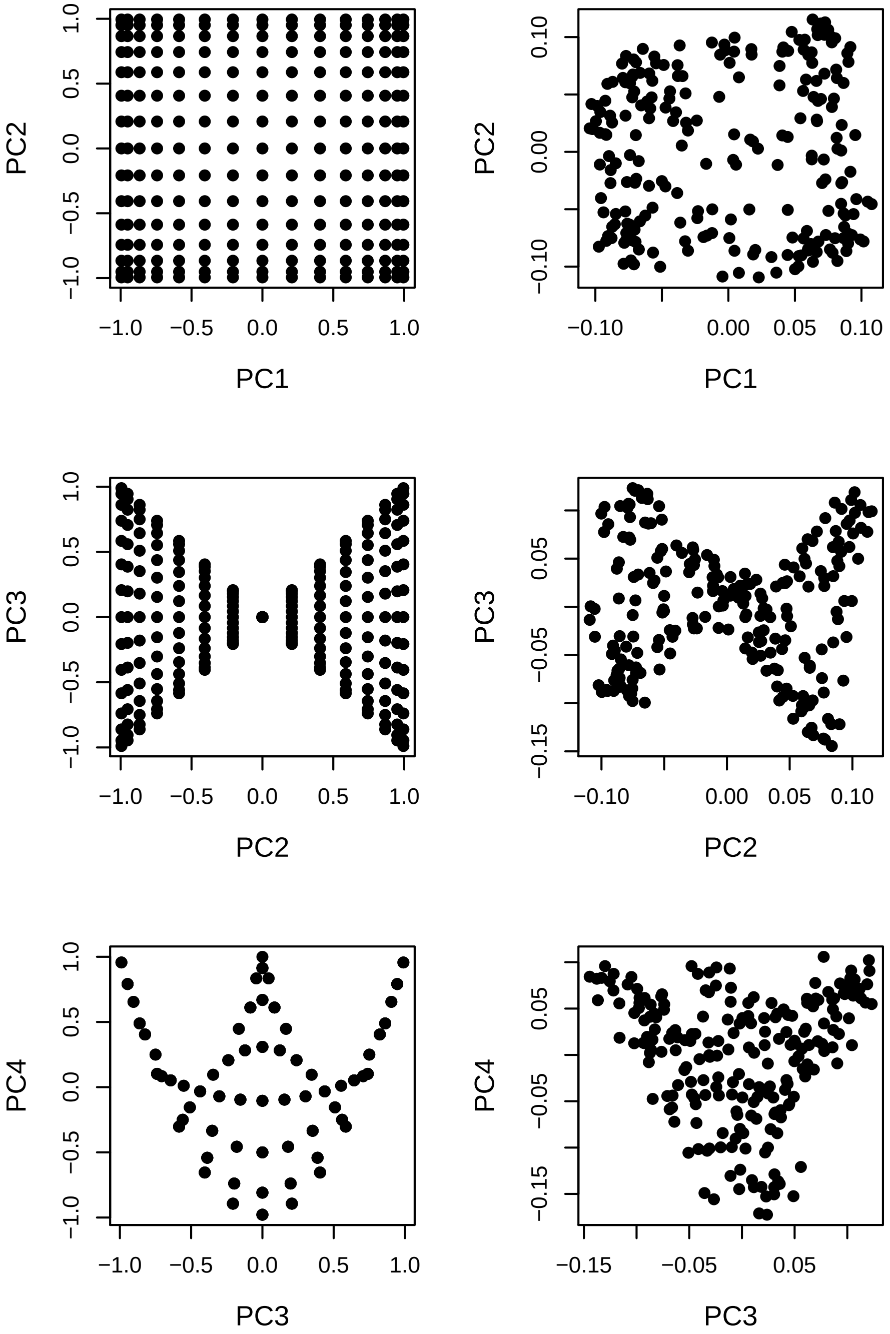

Figure S5: **Example of biplots of PCs from 2-dimensional spatial data.** The left-hand column contains biplots of the 4 idealized PCs expected from the DCT. The right-hand column contains biplots of the 4 observed PCs from data from a stepping-stone model simulation (same simulated data as in fig. 1 of main text, i.e. $4Nm = 0.1$, $D_s = 225$ (i.e., 15×15), $D = 961$ (i.e., 31×31), $n = 200$, and $L = 500$.)

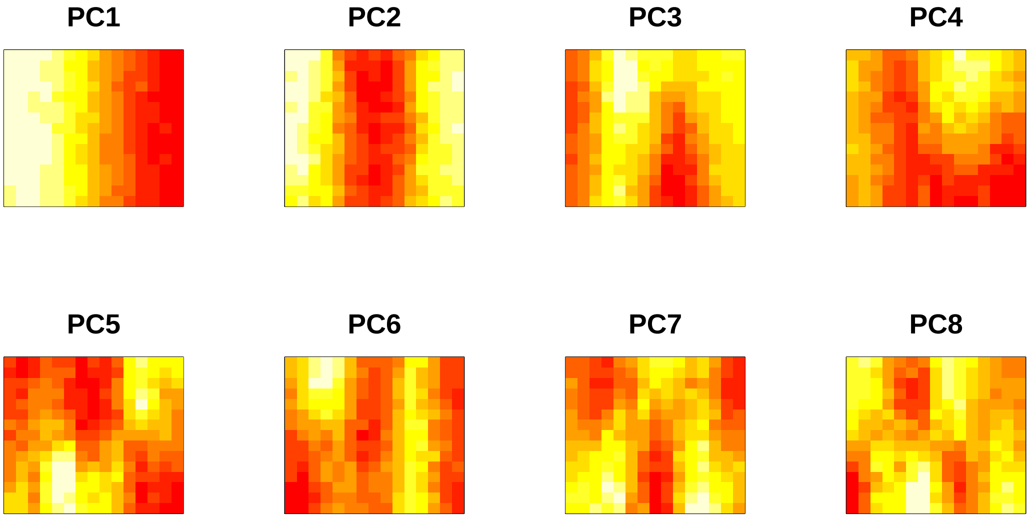

Figure S6: **Plots of PC-maps for PC1-PC8 from a two-dimensional stepping-stone simulation where $4Nm = 0.1$ in one dimension ("east-west") and $4Nm = 1$ in the other ("north-south").** The PCs no longer show the four canonical shapes, but they still have clear sinusoidal patterns. For example PC2 is analogous to the DCT basis function with $u = 0$,$v = 2$ (fig. S4). Additional parameters for these simulations are: $D_s = 225$ (i.e., 15×15), $D = 961$ (i.e., 31×31), $n = 200$, and $L = 500$.

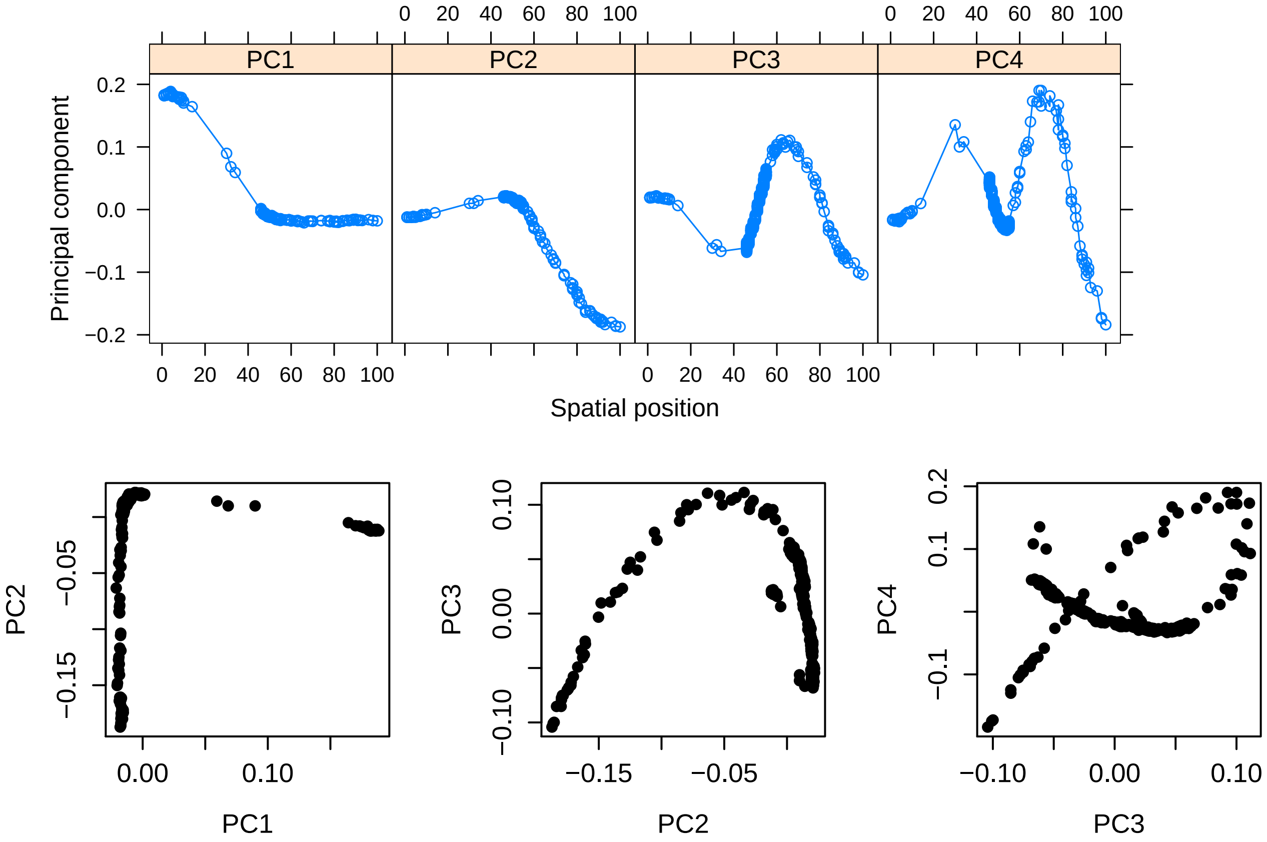

Figure S7: **An example of the distortion of idealized PCs due to biased spatial sampling.** 500 individuals are sampled from a habitat of 100 demes arranged along in a line and genotyped at 500 polymorphic sites. The effective migration parameter is set to $4Nm = 1$. The sampling distribution is biased towards sampling individuals in the center of the habitat and then sampling out to the edges of the habitat but with an added bias towards sampling one end of the habitat slightly more than the other.

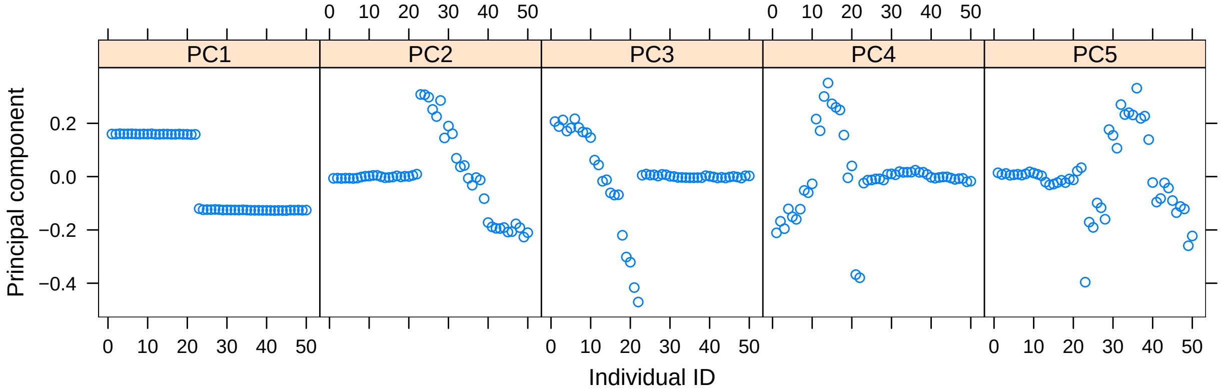

Figure S8: **An example of PCs from a sample with discrete and continuous patterns of variation.** Fifty individuals were drawn at random from one of two sampling areas within a habitat consisting of 100 demes arranged in a line and genotyped at 1000 polymorphic loci. The individual IDs reflect the order of individuals habitat. The first 22 individuals are from area 1 (the first ten demes in the linear array of demes) and the last 28 are from region 2 (the last ten demes in the linear array of demes). As one can see, PC1 separates out individuals of the 2 sampling areas. PC2 and PC3 reflects the "linear" component within area 2 and area 1, respectively. PC4 and PC5 are the "distance from the center shape" for area 1 and area 2. For the simulations, $4Nm = 1$.

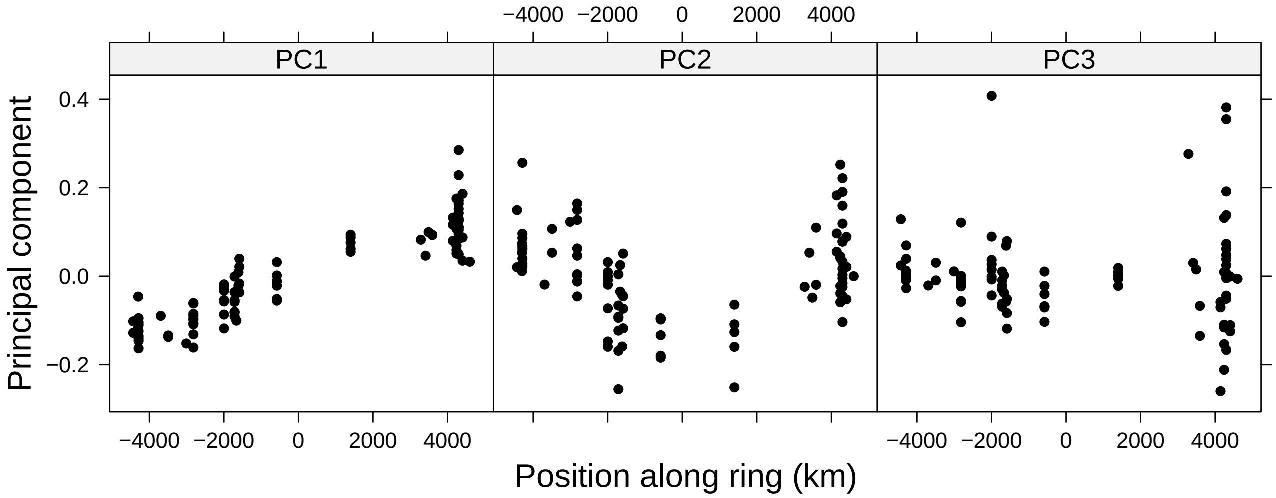

Figure S9: **The first three one-dimensional PC-maps for the *P. trochiloides* data.** Geographic position in this case is equivalent to the position along the ring-shaped habitat.

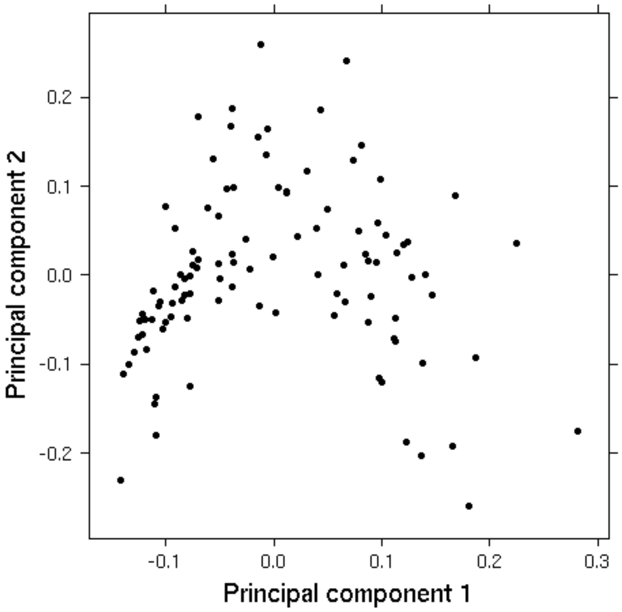

Figure S10: **PC1 vs PC2 for the *P. trochiloides* data.**

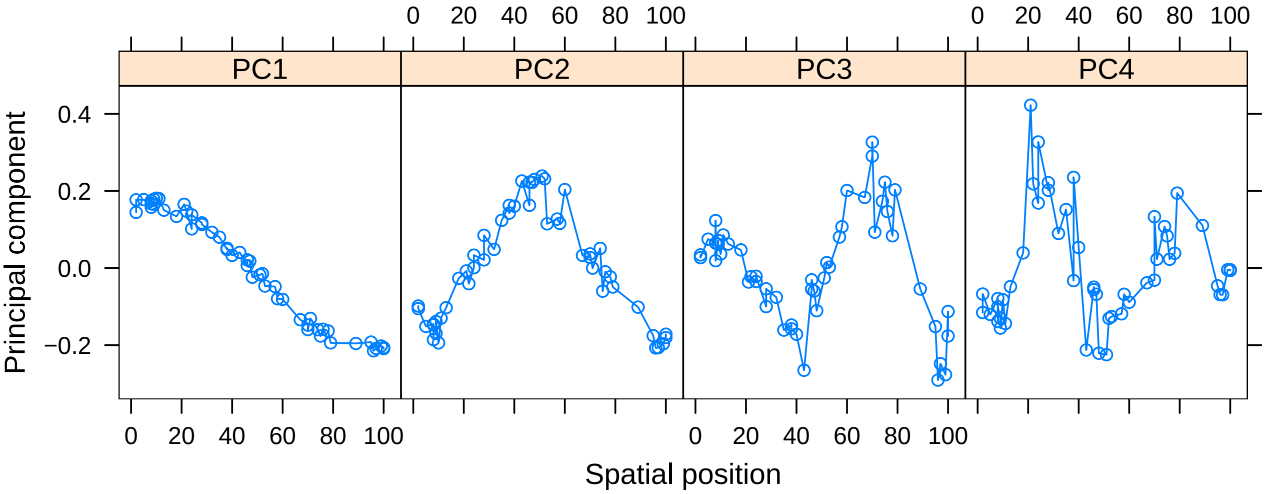

Figure S11: **One-dimensional PC-maps for the same case as in fig. 2 in the main text, but with the effective migration parameter** $4Nm = 100$ **rather than** $4Nm = 1$**.** With increasing effective migration rates, the sinusoidal patterns become more noisy, particularly for higher PCs (e.g. PC4 here). Additional parameters for these individual-based simulations are: $n = 50$, $D = 100$, $n = 1$, and $L = 1000$.

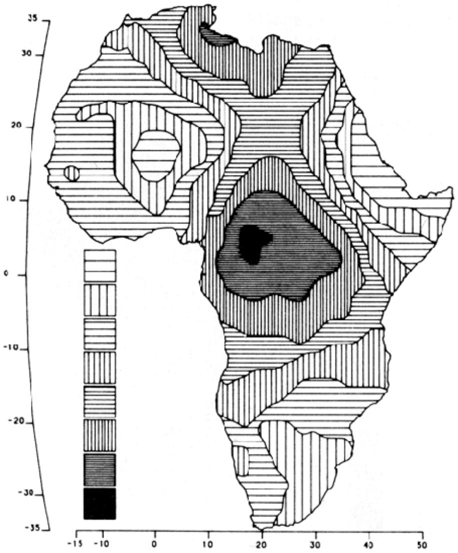

Figure S12: **Example of an original principal component map from [8] (Figure 3.11.4).** This figure is included to allow readers to see the impact of our re-coloring.